 CMES, vol.96, no.4, pp.275-292, 2013

DRBEM Solution of Incompressible MHD Flow with Magnetic Potential

B. Pekmen[1,2], **M. Tezer-Sezgin**[2,3]

Abstract: The dual reciprocity boundary element method (DRBEM) formulation is presented for solving incompressible magnetohydrodynamic (MHD) flow equations. The combination of Navier-Stokes equations of fluid dynamics and Maxwell's equations of electromagnetics through Ohm's law is considered in terms of stream function, vorticity and magnetic potential in 2D. The velocity field and the induced magnetic field can be determined through the relations with stream function and magnetic potential, respectively. The numerical results are visualized for several values of Reynolds (*Re*), Hartmann (Ha) and magnetic Reynolds number (*Rem*) in a lid-driven cavity, and in a channel with a square cylinder. The well-known characteristics of the fluid flow and MHD flow are exhibited. These are the shift of the core region of the flow and the development of the main vortex in the vorticity through the center of the cavity as *Re* increases. An increase in Ha causes Hartmann layers for the flow at the bottom and top walls. Higher values of *Rem* result in circulation of the magnetic potential at the center of the cavity. An increase in *Re* causes symmetric vortices behind the cylinder to elongate through the channel, and an increase in Hartmann number suppresses this elongation.

Keywords: MHD, DRBEM, lid-driven cavity, flow over a cylinder.

1 Introduction

Magnetohydrodynamics (MHD) is a branch of science dealing with the interaction between the electrically conducting fluids and electromagnetic forces. MHD has crucial applications such as MHD generators, plasma confinement, fusion reactors, and designing cooling systems with liquid metals.

The lid-driven cavity flow is chosen as benchmark problem in most of the studies. It has extensive applications in the environmental fluid mechanics. Some of

[1] Department of Mathematics, Atılım University, 06836, Ankara, Turkey
[2] Institute of Applied Mathematics, Middle East Technical University, 06800, Ankara, Turkey
[3] Department of Mathematics, Middle East Technical University, 06800, Ankara, Turkey

the studies for the solution of Navier-Stokes (NS) equations may be mentioned as follows. The oldest and the most famous study utilizing the implicit multigrid method is the work by Ghia, Ghia, and Shin (1982). Wu and Shao (2004) simulated the incompressible lid-driven cavity flow using parallel lattice Boltzmann method with multi-relaxation time scheme. Ghadi, Ruas, and Wakrim (2008) solved the NS equations in terms of stream function-vorticity using piecewise linear finite element method (FEM). As a test problem, Tsai, Young, and Hsiang (2011) applied the localized differential quadrature method to the lid-driven cavity flow with various Reynolds numbers.

A vast amount of numerical approaches are also carried out on the combination of NS and Maxwell's equations in rectangular ducts. In Sterl (1990), a fast Poisson solver is used to visualize the MHD flow in ducts. Boundary element method deriving a fundamental solution for the convection-diffusion type equations is applied to steady MHD duct flow under the effect of an oblique magnetic field in Bozkaya and Tezer-Sezgin (2007). The coupled equations in terms of velocity and magnetic field for unsteady MHD flow through a rectangular pipe is also solved by finite volume spectral element method in Shakeri and Dehghan (2011).

Incompressible MHD flow studies have also gained much importance in the last decade. For the governing equations of this problem, Armero and Simo (1996) analyzed the long-term dissipativity and unconditional non-linear stability of time scheme algorithms using the Galerkin mixed FEM. A stabilized FEM application is examined in 3D incompressible MHD by Salah, Soulaimani, Habashi, and Fortin (1999). Kang and Keyes (2008) compared the approaches, which are stream function formulation and a hybrid formulation with velocity and magnetic field components, using FEM with an implicit time scheme. Considering the magnetic pressure as a new unknown, Codina and Silva (2006) also employed a stabilized FEM to solve the incompressible MHD flow problem. In 2D, stabilized FEM with different stabilization techniques are applied to solve the incompressible MHD equations in Gerbeau (2000), and in Aydin, Neslitürk, and Tezer-Sezgin (2010). Bozkaya and Tezer-Sezgin (2011) utilized DRBEM for the solution of incompressible MHD equations for Hartmann number values up to 100.

Navier-Stokes equations are also solved in a channel including a square cylinder as a test problem. The flow around an obstacle (circular/rectangular) in a channel has become a prominent physical problem due to its various applications in engineering such as building aerodynamics, flow meters, electronic cooling, heat exchange systems. An old, experimental and numerical investigation for flow past a rectangular cylinder is analyzed in Davis, Moore, and Purtell (1984). In the following year, Yoshida and Nomura (1985) solved the same test problem using FEM adopting a unique direct time integration. Mukhopadhyay, Biswas, and Sundararajan (1992)

also investigated the confined wakes behind a square cylinder in a channel dividing the domain into Cartesian cells and using staggered grids. Later, Breuer, Bernsdorf, Zeiser, and Durst (2000) used two different numerical schemes which are lattice-Boltzmann and finite volume method (FVM) to ensure the reliability of the computations for the flow around a square cylinder. RamŠak, Škerget, Hriberšek, and Žunič (2005) concentrated on a subdomain BEM technique with linear mixed elements applying it to the flow past a cylinder as a test problem. Zhang and Zhang (2012) used the numerical manifold method based on Galerkin-weighted residuals method for the solution of the incompressible flow over a square cylinder with low Reynolds numbers. A parallel DRBEM solution to thermoelasticity and thermoviscoelasticity problems is proposed in the study of Koyuncu, Ikikat, Icoz, Baranoglu, and Yazici (2012).

In this study, incompressible MHD flow equations are solved numerically using DRBEM. The non-dimensional governing equations in terms of stream function, magnetic potential and vorticity provide one to satisfy the divergence free conditions of velocity and induced magnetic field. DRBEM is a computationally cheap method with respect to other domain discretization methods due to its boundary only nature. Further, the space derivatives in convection or reaction terms and the unknown boundary conditions of vorticity may be easily calculated by the DRBEM coordinate matrix. Famous benchmark problems as lid-driven cavity flow and flow past a square cylinder are chosen as test problems. Effects of the variations of the problem parameters on the flow and magnetic potential are shown graphically.

2 Mathematical Basis

The two-dimensional, laminar, incompressible MHD flow in terms of magnetic potential is considered. The fluid is viscous and electrically conducting. The displacement and convection currents, and Hall effect are neglected.

MHD equations are a combination of Navier-Stokes and Maxwell's equations of fluid dynamics and electrodynamics, respectively. With the interaction of the external magnetic field and electrically conducting fluid, an induced current B inside the fluid is generated.

Continuity and momentum equations for an incompressible and electrically conducting fluid are [Davidson (2001)]

$$\nabla.\mathbf{u} = 0 \tag{1}$$

$$\nu\nabla^2\mathbf{u} = \frac{\partial \mathbf{u}}{\partial t} + \mathbf{u}(\nabla.\mathbf{u}) + \frac{1}{\rho_0}\nabla P - \mathbf{J}\times\mathbf{B}, \tag{2}$$

where $\mathbf{u}$ is the velocity field, ν is the kinematic viscosity, P is the pressure, ρ_0 is

the reference density, $\mathbf{B} = (B_x, B_y)$ is the magnetic field and $\mathbf{J}$ is the current density. The last term is the Lorentz force due to the externally applied magnetic field.

Substituting the Ampere's law ($\nabla \times \mathbf{B} = \mu_m \mathbf{J}$) instead of the current density $\mathbf{J}$ in the Lorentz force term, the momentum equations for each velocity component may be written explicitly as

$$\nu \nabla^2 u = \frac{\partial u}{\partial t} + u\frac{\partial u}{\partial x} + v\frac{\partial u}{\partial y} + \frac{1}{\rho_0}\frac{\partial P}{\partial x} + \frac{B_y}{\rho_0 \mu_m}\left(\frac{\partial B_y}{\partial x} - \frac{\partial B_x}{\partial y}\right) \tag{3}$$

$$\nu \nabla^2 v = \frac{\partial v}{\partial t} + u\frac{\partial v}{\partial x} + v\frac{\partial v}{\partial y} + \frac{1}{\rho_0}\frac{\partial P}{\partial y} - \frac{B_x}{\rho_0 \mu_m}\left(\frac{\partial B_y}{\partial x} - \frac{\partial B_x}{\partial y}\right), \tag{4}$$

where μ_m is the magnetic permeability of the fluid.

Once the curl of both sides of Ampere's Law ($\nabla \times \mathbf{B} = \mu_m \mathbf{J}$) and Ohm's Law ($\mathbf{J} = \sigma(\mathbf{E} + \mathbf{u} \times \mathbf{B})$) are taken using the identity $\nabla \times (\nabla \times \mathbf{B}) = \nabla(\nabla.\mathbf{B}) - \nabla^2 \mathbf{B}$, the following magnetic field relation is derived as

$$-\frac{1}{\mu_m}\nabla^2 \mathbf{B} = \sigma(\nabla \times \mathbf{E} + \nabla \times (\mathbf{u} \times \mathbf{B})). \tag{5}$$

Using the Faraday's Law ($\nabla \times \mathbf{E} = -\partial \mathbf{B}/\partial t$) in this relation, the magnetic induction equations for each components may be written as

$$\frac{1}{\sigma \mu_m}\nabla^2 B_x = \frac{\partial B_x}{\partial t} + u\frac{\partial B_x}{\partial x} + v\frac{\partial B_x}{\partial y} - B_x\frac{\partial u}{\partial x} - B_y\frac{\partial u}{\partial y} \tag{6}$$

$$\frac{1}{\sigma \mu_m}\nabla^2 B_y = \frac{\partial B_y}{\partial t} + u\frac{\partial B_y}{\partial x} + v\frac{\partial B_y}{\partial y} - B_x\frac{\partial v}{\partial x} - B_y\frac{\partial v}{\partial y}, \tag{7}$$

where σ is the electrical conductivity of the fluid.

In order to satisfy the continuity condition $\nabla.\mathbf{u} = 0$ and the solenoidal nature of $\nabla.\mathbf{B} = 0$, the two-dimensional stream function ψ and magnetic potential A are defined as

$$u = \frac{\partial \psi}{\partial y}, \quad v = -\frac{\partial \psi}{\partial x} \tag{8}$$

$$B_x = \frac{\partial A}{\partial y}, \quad B_y = -\frac{\partial A}{\partial x}. \tag{9}$$

Substitution of Eq. (8) into the definition of vorticity $w = \partial v/\partial x - \partial u/\partial y$ gives the stream function equation as $\nabla^2 \psi = -w$. Furthermore, the vorticity transport equation is obtained by differentiating Eq.(4) with respect to x, and Eq.(3) with respect to y, and subtracting from each other utilizing the continuity condition $\nabla.\mathbf{u} = 0$

while pressure terms are eliminated. Using Eq. (9) and $\nabla.\mathbf{B} = 0$ in either one of the equations (6) or (7), the magnetic potential equation is obtained as

$$\frac{1}{\sigma\mu_m}\nabla^2 A = \frac{\partial A}{\partial t} + u\frac{\partial A}{\partial x} + v\frac{\partial A}{\partial y}. \tag{10}$$

For the nondimensionalization of the equations, the dimensionless variables are defined as

$$x' = \frac{x}{L},\ y' = \frac{y}{L},\ u' = \frac{u}{U_0},\ v' = \frac{v}{U_0},\ t' = \frac{tU_0}{L} \tag{11a}$$

$$w' = \frac{wL}{U_0},\ \psi' = \frac{\psi}{UL},\ A' = \frac{A}{B_0 L},\ B'_x = \frac{B_x}{B_0},\ B'_y = \frac{B_y}{B_0}, \tag{11b}$$

where L is the characteristic length, U_0 is the characteristic velocity, B_0 is the magnitude of the externally applied magnetic field and t is the time. These dimensionless variables are used in the stream function, vorticity transport and magnetic potential equations, and then the prime notation is dropped. Thus, the nondimensional governing equations in terms of stream function ψ, vorticity w, and magnetic potential A are

$$\nabla^2\psi = -w \tag{12a}$$

$$\frac{1}{Rem}\nabla^2 A = \frac{\partial A}{\partial t} + u\frac{\partial A}{\partial x} + v\frac{\partial A}{\partial y} \tag{12b}$$

$$\begin{aligned}\frac{1}{Re}\nabla^2 w = {} & \frac{\partial w}{\partial t} + u\frac{\partial w}{\partial x} + v\frac{\partial w}{\partial y} \\ & - \frac{Ha^2}{ReRem}\left[B_x\frac{\partial}{\partial x}\left(\frac{\partial B_y}{\partial x} - \frac{\partial B_x}{\partial y}\right) + B_y\frac{\partial}{\partial y}\left(\frac{\partial B_y}{\partial x} - \frac{\partial B_x}{\partial y}\right)\right],\end{aligned} \tag{12c}$$

where the dimensionless parameters are the Reynolds number $Re = UL/\nu$, the magnetic Reynolds number $Rem = UL\sigma\mu_m$, and the Hartmann number $Ha = B_0 L\sqrt{\sigma/\mu}$.

3 DRBEM Application

DRBEM treats all the terms apart from the Laplacian (including nonlinearities) as inhomogeneities, which makes possible to use fundamental solution of Laplace equation. The key idea is to transform all the domain integrals to the corresponding boundary integrals utilizing an approximation (formed by radial basis functions) for inhomogeneities, and a relation between particular solution of Laplace equation and the radial basis functions.

Eqs.(12) are rewritten first as coupled Poisson equations

$$\begin{aligned}
&\nabla^2\psi = b_1(w)\\
&\nabla^2 A = b_2(x,y,t,u,v,A_x,A_y,A_t)\\
&\nabla^2 w = b_3(x,y,t,u,v,w_x,w_y,w_t,B_x,B_y).
\end{aligned} \tag{13}$$

In DRBEM, an approximation for the source term b (here b_1, b_2 or b_3) is proposed as Partridge, Brebbia, and Wrobel (1992)

$$b_i \approx \sum_{j=1}^{N+L} \alpha_j f_{ij} \tag{14}$$

where N is the number of boundary nodes, L is the number of internal collocation points, α_j's are sets of initially unknown coefficients, and the f_{ij}'s are approximating functions which depend on radial distance $r_{ij} = \sqrt{(x_i - x_j)^2 + (y_i - y_j)^2}$, $i, j = 1, 2, \ldots, N+L$ in which i and j correspond to the source(fixed) and the field(variable) points, respectively.

For each source node i, the following integral equation is obtained by applying DRBEM [Partridge, Brebbia, and Wrobel (1992)]

$$c_i\varphi_i + \int_\Gamma \varphi \frac{\partial u^*}{\partial n} d\Gamma - \int_\Gamma \frac{\partial \varphi}{\partial n} u^* d\Gamma = \sum_{j=1}^{N+L} \alpha_j \left(c_i \hat{u}_{ij} + \int_\Gamma \hat{u}_j \frac{\partial u^*}{\partial n} d\Gamma - \int_\Gamma \hat{q}_j u^* d\Gamma \right) \tag{15}$$

where φ denotes either ψ, A or w, $u^* = \frac{1}{2\pi} \ln\left(\frac{1}{r}\right)$ is the fundamental solution of Laplace equation, $c_i = 0.5$ if the boundary Γ is a straight line, and $c_i = 1$ when node i is inside. The relation between the particular solution $\hat{u}_j$ and the approximating function f_j (for axi-symmetric case) is

$$\frac{1}{r}\frac{\partial}{\partial r}\left(r \frac{\partial \hat{u}_{ij}}{\partial r} \right) = \nabla^2 \hat{u}_{ij} = f_{ij}, \qquad i, j = 1, 2, \ldots, N+L. \tag{16}$$

Matrix-vector equations resulting from the discretization of these boundary integrals using linear boundary elements corresponding to stream function, magnetic potential and vorticity equations may be expressed as

$$H\varphi - G\varphi_q = \left(H\hat{U} - G\hat{Q}\right)\alpha, \tag{17}$$

where H and G are BEM matrices containing the boundary integrals of u^* and $q^* = \partial u^*/\partial n$ evaluated at the nodes, respectively, the vectors $\varphi_q = \partial\varphi/\partial n$ contain the known and unknown information at the nodes about normal derivatives of ψ, A

or w. $\hat{U}$ and $\hat{Q}$ are constructed from $\hat{u}_j$ and then $\hat{q}_j = \partial \hat{u}_j / \partial n$ columnwise, and are matrices of size $(N+L)\times(N+L)$. The vector α is deduced from the Eq.(14) as $\alpha = F^{-1}b$, where F is the $(N+L)\times(N+L)$ coordinate matrix containing radial basis functions f_j's as columns evaluated at $N+L$ points.

By using coordinate matrix F for evaluating the space derivatives in b and the backward-Euler formula for the time derivatives, the iteration with respect to time is carried between the system of equations for ψ, A and w as

$$H\psi^{m+1} - G\psi_q^{m+1} = -Sw^m \tag{18}$$

$$u^{m+1} = D_y\psi^{m+1}, \quad v^{m+1} = -D_x\psi^{m+1} \tag{19}$$

$$\left(H - \frac{Rem}{\Delta t}S - RemSM\right)A^{m+1} - GA_q^{m+1} = -\frac{Rem}{\Delta t}SA^m \tag{20}$$

$$B_x^{m+1} = D_yA^{m+1}, \quad B_y^{m+1} = -D_xA^{m+1} \tag{21}$$

$$\left(H - \frac{Re}{\Delta t}S - ReSM\right)w^{m+1} - Gw_q^{m+1} = -\frac{Re}{\Delta t}Sw^m - \frac{Ha^2}{Rem}S\left[\{B_x\}_d^{m+1}D_x\xi + \{B_y\}_d^{m+1}D_y\xi\right] \tag{22}$$

where

$$S = \left(H\widehat{U} - G\widehat{Q}\right)F^{-1}, \quad D_x = \frac{\partial F}{\partial x}F^{-1}, \quad D_y = \frac{\partial F}{\partial y}F^{-1}$$

$$M = \{u\}_d^{m+1}D_x + \{v\}_d^{m+1}D_y, \quad \xi = \left(D_xB_y^{m+1} - D_yB_x^{m+1}\right),$$

and $\{u\}_d, \{v\}_d, \{B_x\}_d, \{B_y\}_d$ enter into the system as diagonal matrices of size $(N+L)\times(N+L)$. Once the shuffling of known and unknown nodal values is done, the reduced systems of the form $Cx = b$ are solved by Gaussian elimination with partial pivoting.

Initially, w^0 and A^0 are taken as zero everywhere except on the boundary. Stream function Eq. (18) is solved using m-th time level values of vorticity w. The velocity components are computed by Eq. (19), and then their boundary conditions are inserted. The magnetic potential at $(m+1)$-th time level is found using Eq. (20). Then, the induced magnetic field components are obtained by Eq. (21), and the insertion of their boundary conditions is carried out. Vorticity boundary conditions are found by using the definition of vorticity with the help of coordinate matrix F

$$w = \nabla\times\mathbf{u} = D_xv - D_yu = \frac{\partial F}{\partial x}F^{-1}v - \frac{\partial F}{\partial y}F^{-1}u. \tag{23}$$

Using these boundary conditions for w, vorticity equation (22) is solved at $(m+1)$-

th time level. Iteration continues in this way until the criterion

$$\frac{\left\|\psi^{m+1}-\psi^{m}\right\|_{\infty}}{\left\|\psi^{m+1}\right\|_{\infty}}+\frac{\left\|A^{m+1}-A^{m}\right\|_{\infty}}{\left\|A^{m+1}\right\|_{\infty}}+\frac{\left\|w^{m+1}-w^{m}\right\|_{\infty}}{\left\|w^{m+1}\right\|_{\infty}}<\varepsilon \tag{24}$$

is satisfied where $\varepsilon = 1e-4$ is the tolerance for the steady-state solution ψ, A and w, respectively. Transient level solution can also be obtained at any time value $t_m = m\Delta t$.

4 Numerical Results

In the computations, the radial basis functions are chosen as $f = 1+r$. Further, $16-$point Gaussian quadrature is used for the integrals in H and G matrices. In order to validate the present method, the $|\psi_{\min}|$ values for an incompressible flow in a lid-driven cavity are given in Tab. 1. As can be seen, the results using considerably small number of grid points are in good agreement with the results in Ghia, Ghia, and Shin (1982).

Table 1: $|\psi_{\min}|$ values of streamlines of Navier-Stokes flow in a lid-driven cavity.

	Present		Ghia, Ghia, and Shin (1982)	
Re	Mesh pts.	$\lvert\psi_{\min}\rvert$	Mesh pts.	$\lvert\psi_{\min}\rvert$
100	17×17	0.1034	129×129	0.1034
400	41×41	0.1135	257×257	0.1139
1000	55×55	0.1140	129×129	0.1179

4.1 Case 1. Lid-Driven Cavity Flow

The electrically conducting fluid is moving down the channel with a pressure gradient and an imposed magnetic fields is in the $+y$-direction which is also perpendicular to the axis of the channel (z-axis). The flow is fully developed, thus the cross-section of the channel is taken as the domain of the problem (lid-driven cavity).

The problem geometry is given in Fig. 1. Stream function and velocity component v are all zero on the walls, and the top wall is moving with a velocity $u = 1$. Magnetic potential is $A = -x+k$ on the walls due to the y-component of external magnetic field $B_0 = (0,1)$, and the constant k is taken as zero similar to the stream function on the boundary. In general, 120 linear boundary elements and 841 interior points are used for this case. Since implicit time integration scheme is used, time increment Δt can be taken not too small.

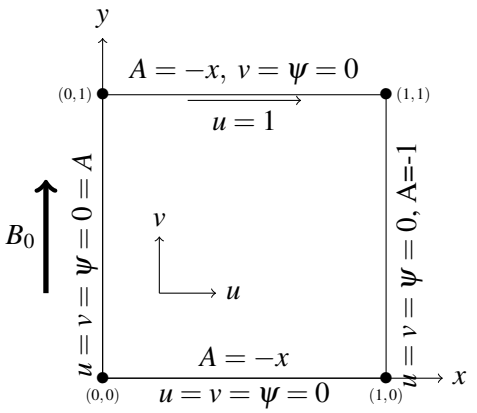

Figure 1: Configuration of the Lid-Driven Cavity Flow.

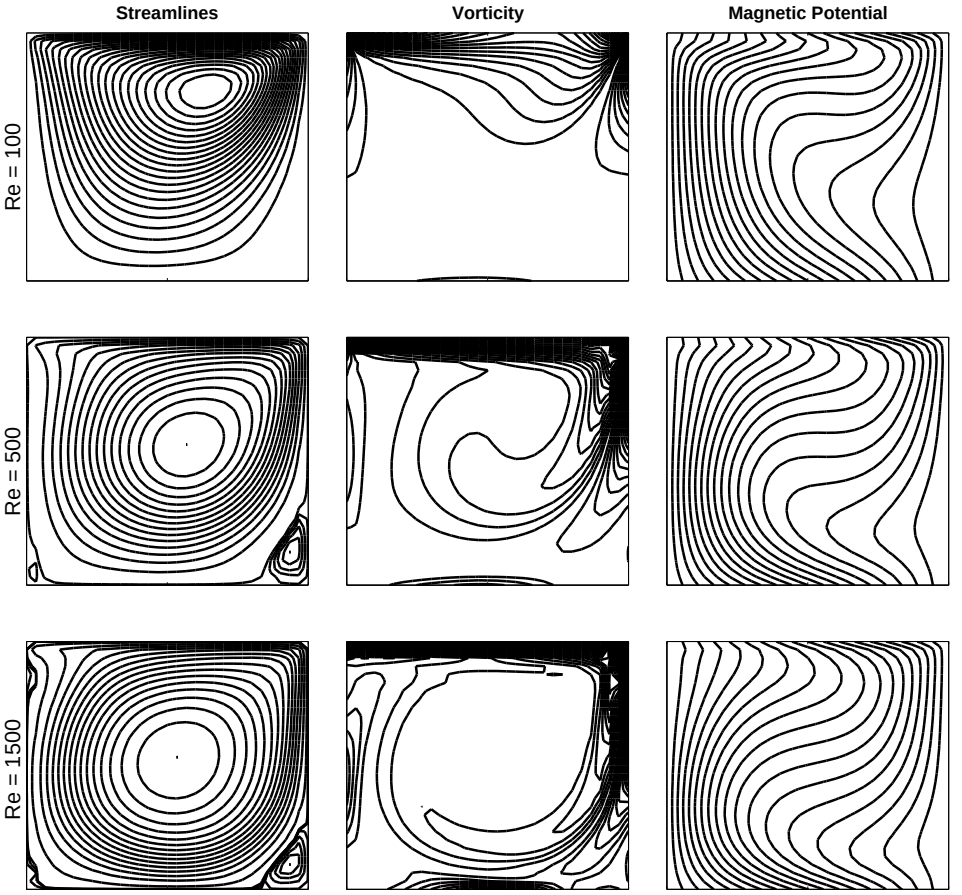

Figure 2: $Rem = 100$, $Ha = 10$, $\Delta t = 0.25$.

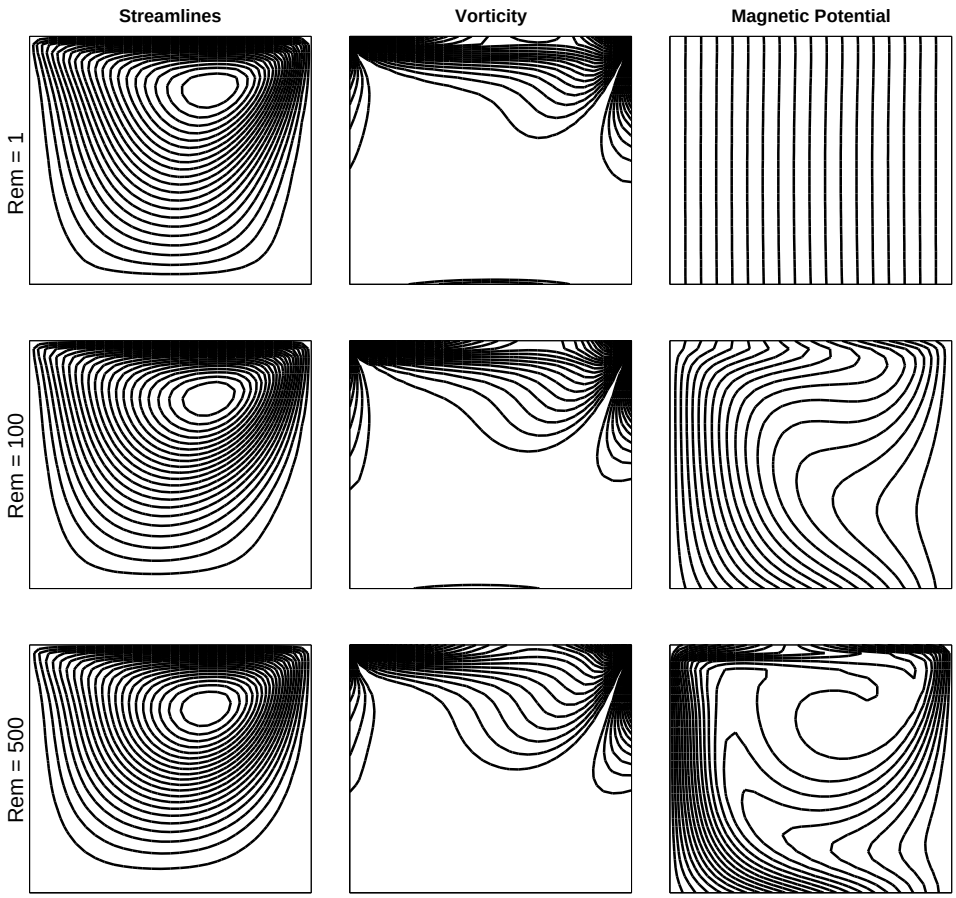

Figure 3: $Re = 100$, $Ha = 10$, $\Delta t = 0.1$.

The center of streamlines which is in the direction of moving lid for small *Re* numbers shifts through the center of the cavity forming new eddies at the lower corners of the cavity as *Re* increases. The circulation of vorticity is pronounced for large values of *Re*. These are the expected behaviors for a lid-driven cavity MHD flow for fixed *Rem* and Ha as can be seen from Fig.2. Magnetic potential lines are not affected much with the variation of *Re*.

The variation in magnetic Reynolds number causes the magnetic potential lines to circulate inside the cavity due to the dominance of convection terms in magnetic potential equation as *Rem* gets larger. Not much alteration occurs in streamlines and vorticity (Fig.3).

Vorticity becomes stagnant at the center clustering through the walls as Ha in-

creases (Fig.4). Thin boundary layers (side layers) and Hartmann layers, respectively, on perpendicular and parallel walls to the direction of B_0, are well observed with an increase in Ha in streamlines. Magnetic potential lines become perpendicular to the top and bottom walls pointing to the decrease in convection terms of magnetic potential equation due to the decrease in velocities, and also, they obey the direction of the externally applied magnetic field as Ha increases. Since the reaction term dominates in vorticity transport equation for large value of $Ha = 100$, a relaxation parameter $0 < \gamma = 0.1 < 1$ is used as $w^{m+1} = \gamma w^{m+1} + (1-\gamma)w^m$ to accelerate the convergence of vorticity.

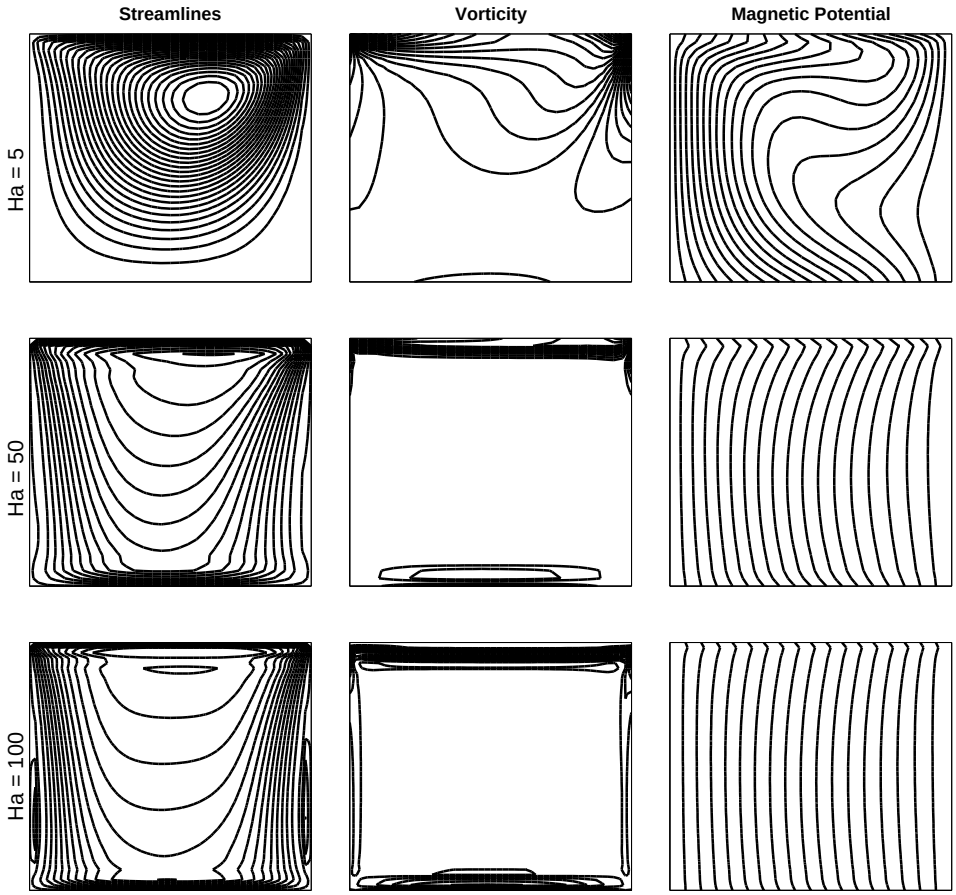

Figure 4: $Re = Rem = 100$, $\Delta t = 0.5, 0.2, 0.1$, for $Ha = 5, 50, 100$.

The magnitude of the velocity of the fluid decreases due to the retarding effect of Lorentz force in the presence of high magnetic field intensity B_0. This is confirmed

by the centerline velocity components as Ha increases in Fig.5. This is the well-known flattening tendency of the MHD flow [Shercliff (1965)].

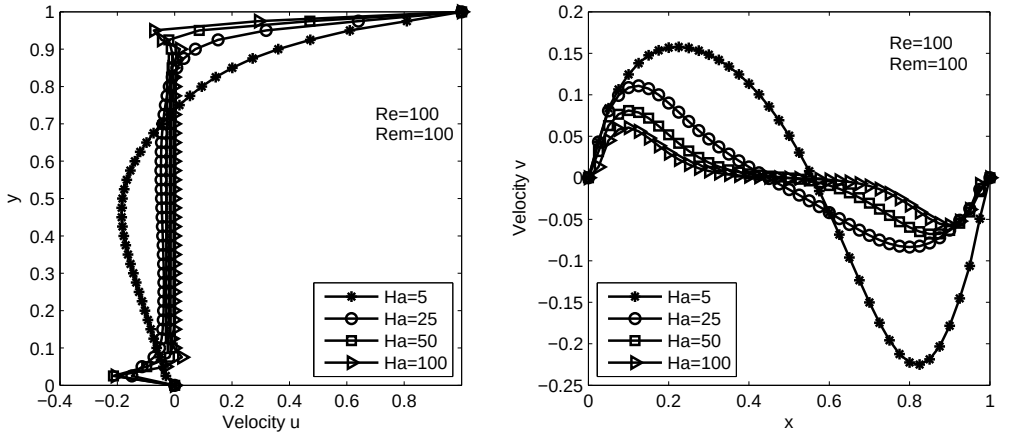

Figure 5: Velocity profiles at mid-sections of the cavity with various Ha.

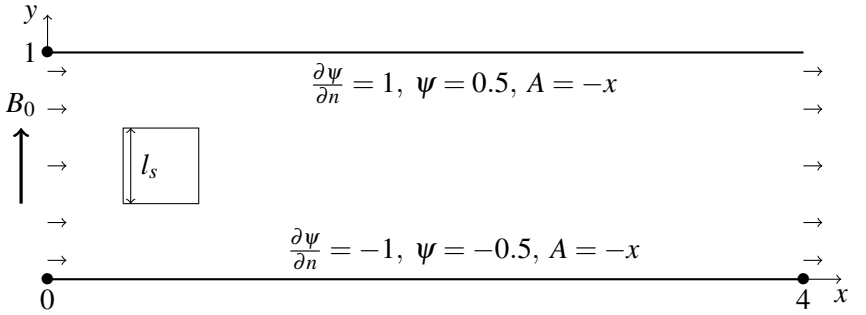

Figure 6: Configuration of the MHD flow past a square cylinder.

4.2 Case 2. Flow over a Square Cylinder

In this case, the MHD flow around a square cylinder confined in a channel between parallel walls is considered. The inlet velocity profile is uniform, and the flow in the far field is also assumed to be a uniform flow ($u = 1$). The behaviors of the flow and magnetic potential are investigated around the square cylinder under the influence of an externally applied magnetic field which is in $+y$-direction.

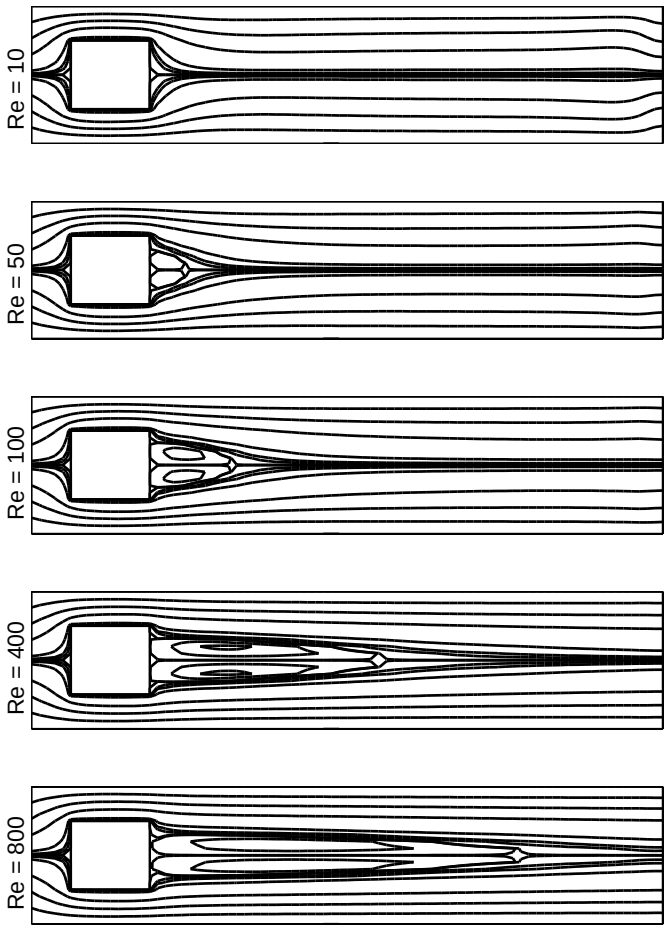

Figure 7: Streamlines at steady-state, $Rem = 10,\ Ha = 5$.

The problem configuration is given in Fig. 6. The boundary conditions which are also seen on the figure may be written as follows. At the inlet $\psi = y - 0.5,\ w = 0,\ u = 1,\ v = 0,\ A = 0$; at the exit $\partial\psi/\partial n = 0,\ \partial w/\partial n = 0,\ A = -4$; on the square cylinder $u = v = \psi = 0,\ A = -x$, the distance of the left bottom corner of the square cylinder to both the inlet and the bottom wall is 0.25, and $l_s = 0.5$. In the computations, $N = 280$ boundary elements with $L = 1380$ interior points are used.

In Figures 7, 8 and 9, streamline variations with respect to Reynolds and Hartmann numbers, and magnetic potential variation with respect to magnetic Reynolds number are illustrated, respectively. With the increase in *Re* (Fig. 7), symmetric vortices emerge behind the cylinder, and they elongate through $+x$-direction. The increase

in Hartmann number suppress this elongation of vortices behind the cylinder as is seen in Fig. 8. As expected, magnetic potential lines are perturbed in $+x$-direction as *Rem* is increased since external magnetic field is perpendicular to the channel walls where the boundary layers start to develop (Fig. 9).

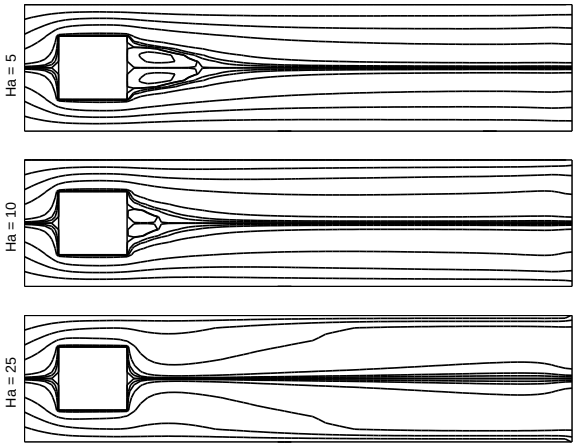

Figure 8: Streamlines at steady-state, $Re = 100,\ Rem = 10$.

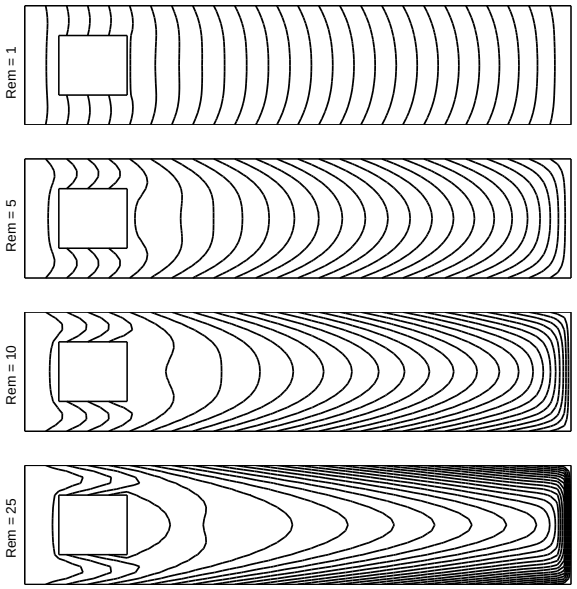

Figure 9: Magnetic potential lines at steady-state, $Re = 100,\ Ha = 5$.

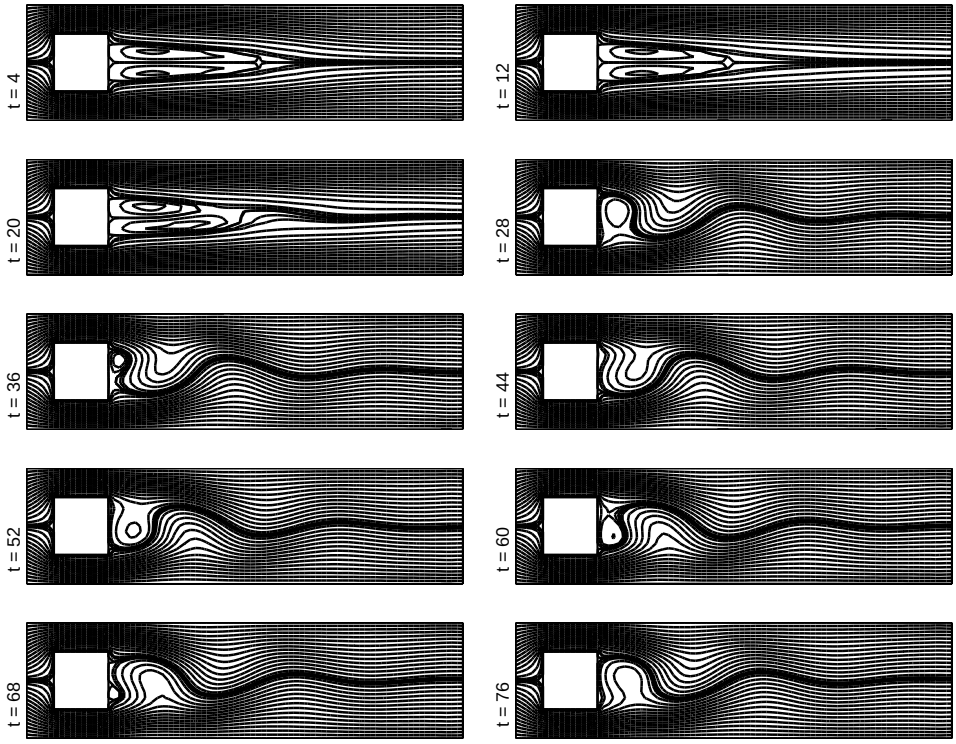

Figure 10: Streamlines at transient levels, $Re = 300,\ Rem = 10,\ Ha = 5$.

In Figs. 10-11, the vortex changes in the streamlines behind the square cylinder at transient levels are reported. As can be seen, the symmetric vortices are shrunk and a periodic behavior of the flow is observed as time passes. As the fluid move away behind the square cylinder, the periodic behavior diminishes and the flow becomes uniform at the exit of the channel. This may be due to the uniform flow field on the channel walls.

5 Conclusion

This study presents the DRBEM solution of incompressible MHD flow in terms of stream function, magnetic potential and vorticity satisfying the divergence free conditions for the velocity and induced magnetic field. The results are visualized as contour maps with respect to varying dimensionless parameters Reynolds, Hartmann and magnetic Reynolds numbers. In lid-driven cavity flow, the increase in Hartmann numbers forms boundary layers through the top and bottom walls, and slows down the fluid motion. Further, magnetic potential lines are enforced to take

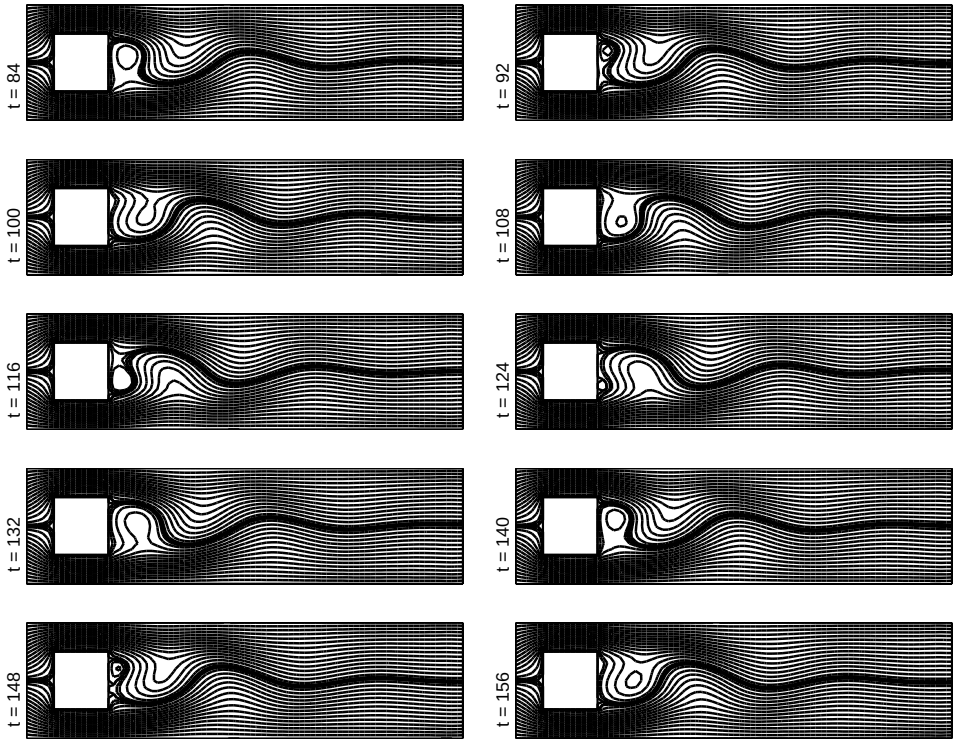

Figure 11: Streamlines at transient levels, $Re = 300,\ Rem = 10,\ Ha = 5$.

the direction of the applied magnetic field as the intensity of external magnetic field is increased. In flow past a square cylinder, even though the vortices behind the cylinder elongate with the increase in *Re*, the retarding effect of Lorentz force causes the symmetric vortices to become smaller, and almost disappear behind the cylinder. Magnetic Reynolds number affects only the magnetic potential lines in both of the test problems.

References

Armero, F.; Simo, J. C. (1996): Long-term dissipativity of time-stepping algorithms for an abstract evolution equation with applications to the incompressible MHD and Navier-Stokes equations. *Computer methods in applied mechanics and engineering*, vol. 131, pp. 41–90.

Aydin, S. H.; Neslitürk, A. I.; Tezer-Sezgin, M. (2010): Two-level finite element method with a stabilizing subgrid for the incompressible MHD equations. *International Journal for Numerical Methods in Fluids*, vol. 62, pp. 188–210.

Bozkaya, C.; Tezer-Sezgin, M. (2007): Fundamental solution for coupled magnetohydrodynamic flow equations. *Journal of Computational and Applied Mathematics*, vol. 203, pp. 125–144.

Bozkaya, N.; Tezer-Sezgin, M. (2011): The DRBEM solution of incompressible MHD flow equations. *International Journal for Numerical Methods in Fluids*, vol. 67, pp. 1264–1282.

Breuer, M.; Bernsdorf, J.; Zeiser, T.; Durst, F. (2000): Accurate computations of the laminar flow past a square cylinder based on two different methods: lattice-boltzmann and finite-volume. *International Journal of Heat and Fluid Flow*, vol. 21, pp. 186–196.

Codina, R.; Silva, H. N. (2006): Stabilizaed finite element approximation of the stationary magneto-hydrodynamics equations. *Computational Mechanics*, vol. 38, pp. 344–355.

Davidson, P. A. (2001): *An Introduction to Magnetohydrodynamics*. Cambridge University Press.

Davis, R. W.; Moore, E. F.; Purtell, L. P. (1984): A numerical-experimental study of confined flow around rectangular cylinders. *Physics of Fluids*, vol. 27, pp. 46–59.

Gerbeau, J. F. (2000): A stabilized finite element method for the incompressible magnetohydrodynamic equations. *Numerische Mathematik*, vol. 87, pp. 83–111.

Ghadi, F.; Ruas, V.; Wakrim, M. (2008): Numerical solution of the time-dependent incompressible Navier-Stokes equations by piecewise linear finite elements. *Journal of Computational and Applied Mathematics*, vol. 215, pp. 429–437.

Ghia, U.; Ghia, K. N.; Shin, C. T. (1982): High-Re solutions for incompressible flow using the Navier-Stokes equations and a multigrid method. *Journal of Computational Physics*, vol. 48, pp. 387–411.

Kang, K. S.; Keyes, D. E. (2008): Implicit symmetrized streamfunction formulations of magnetohydrodynamics. *International Journal for Numerical Methods in Fluids*, vol. 58, pp. 1201–1202.

Koyuncu, M.; Ikikat, F. Y.; Icoz, G. C.; Baranoglu, B.; Yazici, A. (2012): Implementation of a parallel dual reciprocity boundary element method for the solution of coupled thermoelasticity and thermoviscoelasticity problems. *Computer Modeling in Engineering & Sciences(CMES)*, vol. 84, pp. 13–16.

Mukhopadhyay, A.; Biswas, G.; Sundararajan, T. (1992): Numerical investigation of confined wakes behind a square cylinder in a channel. *International Journal for Numerical Methods in Fluids*, vol. 14, pp. 1473–1484.

Partridge, P. W.; Brebbia, C. A.; Wrobel, L. C. (1992): *The dual reciprocity boundary element method*. Computational Mechanics Publications, Elsevier Science.

RamŠak, M.; Škerget, L.; Hriberšek, M.; Žunič, Z. (2005): A multidomain boundary element method for unsteady laminar flow using stream function-vorticity equations. *Engineering Analysis with Boundary Elements*, vol. 29, pp. 1–14.

Salah, N. B.; Soulaimani, A.; Habashi, W. G.; Fortin, M. (1999): A conservative stabilized finite element method for the magneto-hydrodynamic equations. *International Journal for Numerical Methods in Fluids*, vol. 29, pp. 535–554.

Shakeri, F.; Dehghan, M. (2011): A finite volume spectral element method for solving magnetohydrodynamic (MHD) equations. *Applied Numerical Mathematics*, vol. 62, pp. 1–23.

Shercliff, J. A. (1965): *A Textbook of Magnetohydrodynamics*. Pergamon Press.

Sterl, A. (1990): Numerical simulation of liquid-metal MHD flows in rectangular ducts. *Journal of Fluid Mechanics*, vol. 216, pp. 161–191.

Tsai, C. H.; Young, D. L.; Hsiang, C. C. (2011): The localized differential quadrature method for two-dimensional stream function formulation of Navier-Stokes equations. *Engineering Analysis with Boundary Elements*, vol. 35, pp. 1190–1203.

Wu, J.-S.; Shao, Y.-L. (2004): Simulation of lid-driven cavity flows by parallel lattice Boltzmann method using multi-relaxation-time scheme. *International Journal for Numerical Methods in Fluids*, vol. 46, pp. 921–937.

Yoshida, Y.; Nomura, T. (1985): A transient solution method for the finite element incompressible Navier-Stokes equations. *International Journal for Numerical Methods in Fluids*, vol. 5, pp. 873–890.

Zhang, Z.; Zhang, X. (2012): Direct simulation of Low-Re flow around a square cylinder by numerical manifold method for Navier-Stokes equations. *Journal of Applied Mathematics*, vol. 2012.